Mechanistic Toxicity Evaluation of Uncoated and PEGylated Single-Walled Carbon Nanotubes in Neuronal PC12 Cells

Yongbin Zhang,[†] Yang Xu,[‡] Zhiguang Li,[†] Tao Chen,[†] Susan M. Lantz,[†] Paul C. Howard,[†] Merle G. Paule,[†] William Slikker, Jr.,[†] Fumiya Watanabe,[‡] Thikra Mustafa,[‡] Alexandru S. Biris,[‡,*] and Syed F. Ali[†,*]

[†]National Center for Toxicological Research, Food and Drug Administration, 3900 NCTR Road, Jefferson, Arkansas 72079, United States, and [‡]Nanotechnology Center, University of Arkansas at Little Rock, 2801 S. University Avenue, Little Rock, Arkansas 72204, United States

ABSTRACT We investigated and compared the concentration-dependent cytotoxicity of single-walled carbon nanotubes (SWCNTs) and SWCNTs functionalized with polyethylene glycol (SWCNT-PEGs) in neuronal PC12 cells at the biochemical, cellular, and gene expressional levels. SWCNTs elicited cytotoxicity in a concentration-dependent manner, and SWCNT-PEGs exhibited less cytotoxic potency than uncoated SWCNTs. Reactive oxygen species (ROS) were generated in both a concentration- and surface coating-dependent manner after exposure to these nanomaterials, indicating different oxidative stress mechanisms. More specifically, gene expression analysis showed that the genes involved in oxidoreductases and antioxidant activity, nucleic acid or lipid metabolism, and mitochondria dysfunction were highly represented. Interestingly, alteration of the genes is also surface coating-dependent with a good correlation with the biochemical data. These findings suggest that surface functionalization of SWCNTs decreases ROS-mediated toxicological response *in vitro*.

KEYWORDS: single-walled carbon nanotubes · functionalization · toxicity · reactive oxygen species · gene expression

Carbon nanotubes (CNTs) are hollow cylinders made of graphene sheets rolled up to form a tube. On the basis of the numbers of single tubes formed by graphene layers, CNTs are classified as single-walled carbon nanotubes (SWCNTs), double-walled carbon nanotubes (DWCNTs), and multiple-walled carbon nanotubes (MWCNTs). Due to their unique physical, mechanical, and chemical properties, carbon nanotubes have attracted tremendous interest in electronics, optical communications, and energy storage in the past decade.[1−5] SWCNTs, a material with one-dimensional (1D) characteristics and extremely high aspect ratio (generally a diameter of around 0.7−3 nm and lengths of up to several centimeters), elicit different biological behavior compared to spherical nanoparticles when introduced in biological systems. The unique crystalline structure and morphological characteristics of these nanostructures have made them excellent candidates for a number of applications that include photothermal therapy, photoacoustic imaging, drug delivery, and other biomedical applications.[6−9] SWCNTs are relatively flexible and based on their unique morphology have considerable ability to interact with the membranes of cells and to penetrate inside due to a "snaking effect". Recently, we have shown that carbon nanotubes have the ability to penetrate a number of other biological systems ranging from tissues to plant seeds.[10−12] Moreover, their high surface area allows the loading of multiple molecules along the nanotubes' side walls; however, the poor solubility of carbon nanotubes has limited their biomedical applications for many years. Therefore, strategies for surface functionalization of carbon nanotubes have been developed to make CNTs more biocompatible. Two approaches, including covalent and noncovalent functionalization, have been successfully established.[13] SWCNTs can be coated by single-strand DNA *via* $\pi-\pi$ stacking between aromatic DNA base units and the nanotubes' surface;[14] however, DNA molecules noncovalently coated on the surface of SWCNTs can be cleaved by nucleases in serum, thus limiting this approach in biological systems.[15] Another approach is to functionalize the SWCNT with poly(ethylene glycol) (PEG) through covalent functionalization, an approach that has been intensively studied and employed in biomedical applications, since it allows excellent individual dispersion and good stability of the nanotube over a long period of time.[16] Although this approach may affect the surface of

* Address correspondence to Syed.Ali@fda.hhs.gov, asbiris@ualr.edu.

Received for review May 3, 2011 and accepted August 25, 2011.

Published online August 25, 2011
10.1021/nn2016259

SWCNTs and interfere with their optical and electrical properties, covalently functionalized carbon nanotubes show promising applications in a number of biomedical applications such as gene and drug delivery systems.[17]

SWCNTs have tremendous potential for applications in biomedicine.[18−22] For example, a large number of reports have indicated the ability of SWCNTs to deliver both *in vivo* and *in vitro* drug molecules[21] and oncogene suppressor genes[18] to tumors and cells. A significant finding was recently reported that indicates that the graphitic structure of the SWCNTs can be degraded enzymatically[23] and therefore leaves open the possibility that nanomaterials may biodegrade when introduced in various biological systems. However, the single major limitation was related to their possible induced side effects, which need to be thoroughly addressed and studied.[24] On the other hand, evidence for the toxic potential of carbon nanotubes is controversial. Many publications have reported no apparent toxicity,[19,25−31] while there are a number of studies showing biologically significant toxicity *in vitro*[32−37] and *in vivo*.[38−43] The physicochemical characterization of nanomaterials has been recognized as the fundamental aspect for the accurate correlation between the induced toxicological or biological responses and the unique properties of these nanomaterials.[24] The major issues addressed in these toxicological profiles are the purity, dosage, surface chemistry, dimensions, and exposure route of carbon nanotubes used in these studies. Several SWCNT synthesis methods involve the use of metal catalysts (*i.e.*, Fe, Cu, and Mg), which have been known to be toxic to cells or organisms under certain conditions.[44] Such impurities introduced during the process of synthesis or functionalization should be removed from the samples before evaluating the inherent SWCNT toxicity. Current published reports using well-characterized nanomaterials are still limited. An acute and chronic toxicity study using functionalized single-walled carbon nanotubes showed no evidence of toxicity in clinical chemistry and histopathology through intravenous injection of mice, with SWCNTs accumulating in macrophages of liver and spleen over 4 months.[25] By contrast, it has been reported that carbon nanotubes induced granulomas and inflammation after *i.p.* administration in mice, showing asbestos-like pathogenicity.[45] A number of studies have demonstrated that several types of metal nanoparticles (such as silver, copper, and manganese) can deplete dopamine and its metabolites 3,4-dihydroxyphenylacetic acid and homovanillic acid and elicit dopaminergic toxicity in PC12 cells.[46,47] Recent studies have also shown that nanosized carbon nanoparticles can interact with neurons and ultimately translocate to the brain.[48,49] It has been reported that amine-modified, single-walled carbon nanotubes used as scaffolds in neural cells and brain tissues could prevent ischemic injury of neurons in a rat stroke model.[19] Nevertheless, carbon nanotubes have the ability to cross the blood−brain barrier and can accumulate in brain tissue, making therefore the neurotoxicity of CNTs an extremely important issue.[50] This need was recently highlighted by a recent study on the biodistribution of PEGylated SWCNTs that clearly indicated their ability to reach brain tissue. The surface modification of SWCNTs by PEGylation allows a highly individual dispersion of the nanotubes, but also these nanostructures were found to reside for longer periods of time in the blood circulation, making them more prone to reach various organs including the brain.[51]

PC12 cells, derived from pheochromocytoma of the rat adrenal medulla, represent one of the best biological models to study the cytotoxicity and neurotoxicity of any chemicals or nanomaterials. The PC12 cell culture system can synthesize, take up, and release one important neurotransmitter, dopamine, and it has been widely used to screen the potential cytotoxicity and neurotoxicity of the central nervous system to addictive drugs, metals, and pesticides. Recently, this cell model has been successfully used to evaluate the neurotoxin potential and investigate the toxic mechanism of a number of nanomaterials including silica nanoparticles, carbon nanotubes, graphene, quantum dots, iron oxide, silver, and titanium dioxide nanoparticles.[11,47,52−57] Therefore, PC12 cells were selected as a model for this mechanistic toxicity study of the impact of nanotube surface chemistry at cellular and molecular levels.

Recently, we reported that the shape of carbon nanomaterials plays a pivotal role in adversely affecting biological systems.[11] The surface coating of SWCNTs is another important parameter, both for the biological properties of these nanomaterials and their toxic potential. Given the high potential of SWCNT structures to be used as delivery carriers for growth factors, drug molecules, and other proteins for neural reconstruction, regeneration, and photothermal therapy and imaging in the nervous system, it is crucial to understand and study the interaction between such nanomaterials and neuronal cells. Due to their small size, carbon nanotubes may be taken up by cells and possibly cause toxicity. In particular, the mechanism of cellular uptake is not clear since traditional imaging techniques, such as transmission electron microscopy (TEM), generally fail to detect and especially quantify SWCNTs in cells and tissues due to the similar contrast of the SWCNTs and tissues. Due to the strong Raman signature of SWCNTs, Raman spectroscopy was used successfully to detect the uptake and the biodistribution of SWCNTs in tissue culture and *in vivo*.[58] Therefore, the surface functionalization of carbon nanomaterials by PEGylation is proposed to affect the biological behavior in PC12 cells. This study presents an evaluation of the neurotoxicity and

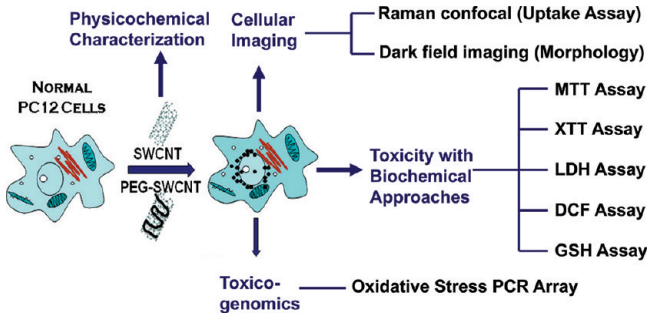

Figure 1. Diagram of the experimental procedure. Single-walled carbon nanotubes (SWCNTs) and PEG-coated SWCNTs (SWCNT-PEGs) were incubated with PC12 cells, and their toxicity was assessed by a combination of biochemical and gene expression approaches.

intracellular distribution/accumulation of both SWCNTs and SWCNT-PEGs and their underlying molecular mechanisms in neuronal PC12 cells. We found that PEG functionalization significantly reduces the side effects of SWCNTs *in vitro* in neuronal PC12 cells, as well as the disturbance of oxidative stress-related gene expression.

RESULTS AND DISCUSSION

Characterizations of SWCNT and SWCNT-PEG. It is critical to perform physical and chemical characterization of nanomaterials before nanotoxicology studies.[59] Figure 2 shows the TEM images of SWCNTs and SWCNT-PEGs. The average diameter of the SWCNTs was in the range 0.7−1.6 nm with a length of 0.2−3 μm and an overall purity in excess of 97%, based on EDS elemental analysis. After chemical functionalization with PEG molecules, the average diameter of SWCNT-PEG samples increased to 2.5−4.5 nm and the length shortened to 0.1−1 μm, clearly indicating the formation of a PEG coating on the SWCNT surface. High-resolution TEM analysis of both the SWCNT and SWCNT-PEG samples indicated the presence of a uniform, thin, noncrystalline film associated with the PEG presence around the nanotubes that had been surface treated. The shape of both SWCNTs and SWCNT-PEGs appears, as expected, to be nanofibrous, and it can be observed that the coating is relatively uniform throughout the entire length of the nanotubes. Microscopy analysis indicated that the carbon nanotubes, before and after PEG coating, were found to be mostly dispersed in the cell medium individually or in few-nanotube bundles.

The physical or chemical properties of the nanomaterials may be altered in biological systems due to the surface protein binding, and the nanotubes' surface charge may affect their interactions with cells or other biological systems. As a result, it is critical to fully understand their surface chemistry in addition to their shape and size, especially when introduced into the medium used for cellular cultures. Therefore, we measured the surface charge of the carbon nanotubes (before and after PEGylation) in cellular media. The zeta potential values of the as-obtained SWCNTs and SWCNT-PEGs were found to have negative polarities of −15.53 and −30.14 mV, respectively, indicating that SWCNT-PEGs are possibly more stable in medium suspension compared to the uncoated SWCNTs. Both species of nanotubes were found to be stable in the cellular media during the duration of the experiments.

To further prove the PEG coating of the nanotubes, we performed Raman scattering analysis, which is a vibrational molecular spectroscopy that can be used to characterize various organic and inorganic materials. It is commonly used to characterize carbon nanotubes, since it provides extremely important information about the structure and purity of such graphitic nanomaterials.[60] The D band and G band are characteristic of the graphitic carbon structures of the SWCNTs. The D band is associated with the defects present in the graphitic structure, and the G band corresponds to the E_{2g} modes (stretching vibrations). After the SWCNT surface was functionalized by PEG groups, it was found that the Raman D band intensity increased. In this case, the relative intensity value of I_D/I_G increased from 0.075 to 0.71, as shown in Figure 2, indicating the presence of more noncrystalline structures on the surface of the SWCNTs. At the same time, the D band shifted to 1585 cm^{-1}, which can be attributed to the PEG polymer coating.[61] This finding showed that the magnitude of the upshift is correlated with the bundles or individual SWCNTs coating with polymer. The low magnitude of upshift would suggest that the SWCNT-PEG sample was composed largely of individually dispersed SWCNTs.

Toxicity Evaluation. Previous studies have shown that CNT nanomaterials elicit toxicity in both cell cultures and rodent models.[32−43] However, SWCNT-PEG, a promising functionalized carbon nanomaterial given its structure and properties, is expected to have potential applications in the nanomedicine field.[22,20] Therefore, the cytotoxicity of SWCNT and SWCNT-PEG was determined using multiple end point evaluation, and the potential toxic mechanism was investigated.

It has been noted that multiple approaches should be used in nanotoxicology evaluation studies.[62] The MTT assay, a commonly employed method to evaluate the adverse effect of nanomaterials in cell

	SWCNT	SWCNT-PEG
TEM Image	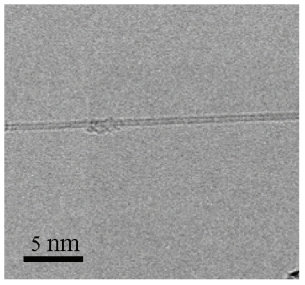	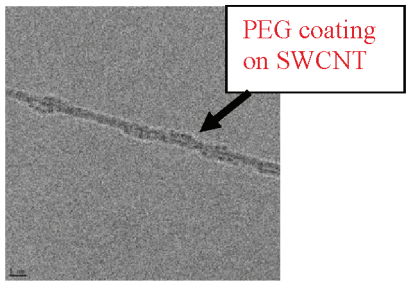
Size Distribution	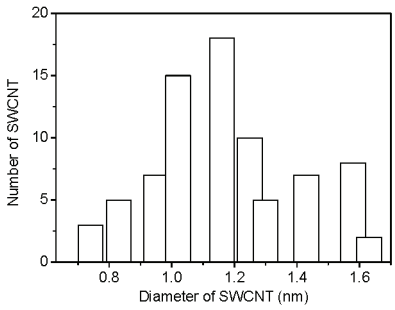	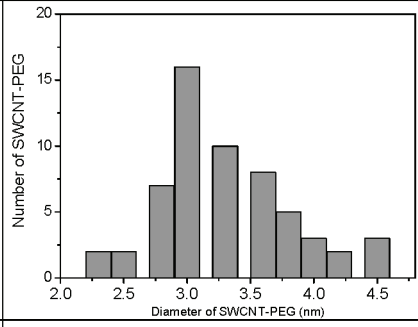
Raman Analysis	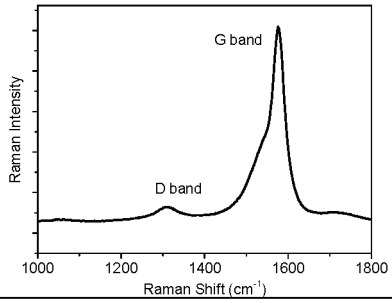	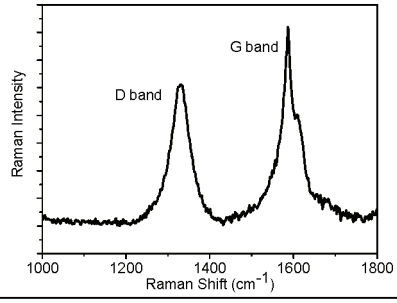
Diameter (nm)	0.7-1.6	2.5-4.5
Length (μm)	0.2-3.0	0.1-1.0
Shape	Fiber like	Fiber like
Zeta Potential (mV in cellular media)	-15.53	-30.14
SWCNT (%)	97.4%	91.2%
Fe, Al, Si (%)	0.22 %, 0.22%, 0.06%	0.00%, 0.03%, 0.00%
Others (% O, N)	2.11%	8.77%

Figure 2. Physical and chemical characterization of SWCNTs and SWCNT-PEGs. The sizes, size distribution, shapes, surface coating, surface charges, and purities were characterized using differential techniques described in the Methods.

culture, was used to measure the mitochondrial function of the cells. However, it has been reported that MWCNTs may affect the MTT assay and sometimes provide false positive results.[63] Coccini *et al*. evaluated the cytotoxicity of MWCNTs by different methods *in vitro* and indicate that MWCNTs appear to interact with tetrazolium salts in the medium, thus reflecting a false positive cytotoxicity.[64] Another study has shown differential cytotoxicity results of MWCNTs by using MTT and WST-1 assays.[65] Therefore, a modified procedure was used in our studies to attempt to avoid the interference. Two additional steps were involved in the MTT testing procedure. CNTs in the medium were extensively washed before adding the MTT solution, and the supernatant was transferred to another plate for reading after centrifugation of the dissolved formazan in the DMSO. It has been reported that the XTT assay is a good approach for MWCNT toxicity evaluation,[63] and thus we verified the mitochondria cytotoxicity by using the XTT assay. In agreement with previous findings,[63] the differential mitochondria toxicity was also observed in our comparative studies involving MTT and XTT assays. It has been reported that the MTT assay is considered one of

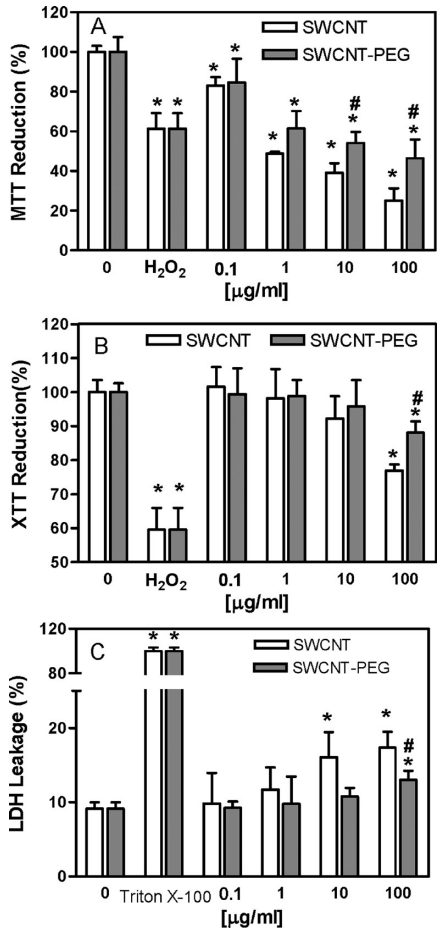

Figure 3. Effect of surface modification of SWCNTs on mitochondrial toxicity and membrane damage evaluated by (A) MTT assay, (B) XTT assay, and (C) LDH release (cell membrane damage marker). Cells were treated with different concentrations of nanomaterials for 24 h. At the end of the incubation period, MTT reduction, XTT reduction, or LDH assays were performed to evaluate the cytotoxicity as described in the Methods section. Data were expressed as mean ± standard error (SE) based on at least triplicate observations from three independent experiments. (*) indicates statistically significant from control; (#) indicates statistically significant within the same concentration group ($p < 0.05$).

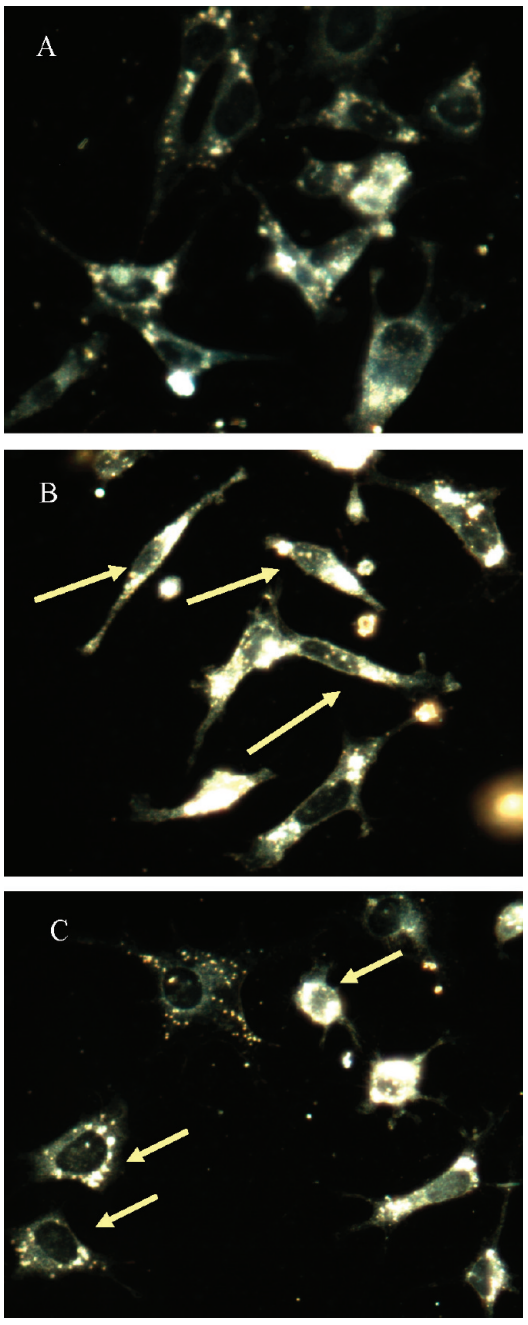

Figure 4. Morphological changes induced by SWCNTs and SWCNT-PEGs in PC12 cells after incubation of the carbon nanotubes for 24 h. (A) Normal morphology of the PC12 cells. (B) SWCNTs appear to induce PC12 cells to form the spindle shape (arrows). (C) SWCNT-PEGs (100 ug/mL) inhibit dendrite growth (arrows).

the most sensitive methods for cytotoxicity evaluation compared with other approaches.[66] However, we could not exclude the possibility that the MTT salts may have interactions with the SWCNTs like MWCNT and produce false positive results. Further investigations need to be conducted, and an evaluation of SWCNT using the MTT assay should be additionally validated by other methods. For the MTT analysis, the metabolic activity of PC12 cells was found to decrease in a concentration-dependent manner after 24 h of exposure to either SWCNT-PEGs or SWCNTs. Cytotoxic effects in the PC12 cells were observed for both the SWCNTs and SWCNT-PEGs at high concentrations (100 μg/mL) using MTT and XTT assays (Figure 3A,B). SWCNT-PEG was found to be significantly less toxic than uncoated SWCNT in high concentration, suggesting that PEG-functionalized SWCNTs possess a higher level of biocompatibility compared to the SWCNTs.

LDH release is a method of measuring the membrane damage, a hallmark of necrosis. In our studies, significant LDH release was noted after 24 h of exposure to 10−100 μg/mL (Figure 3C). Consistent with MTT data, SWCNT-PEGs had a trend to decrease LDH release after functionalization, indicating the less cytotoxic effect of the SWCNT-PEG nanotubes compared to the

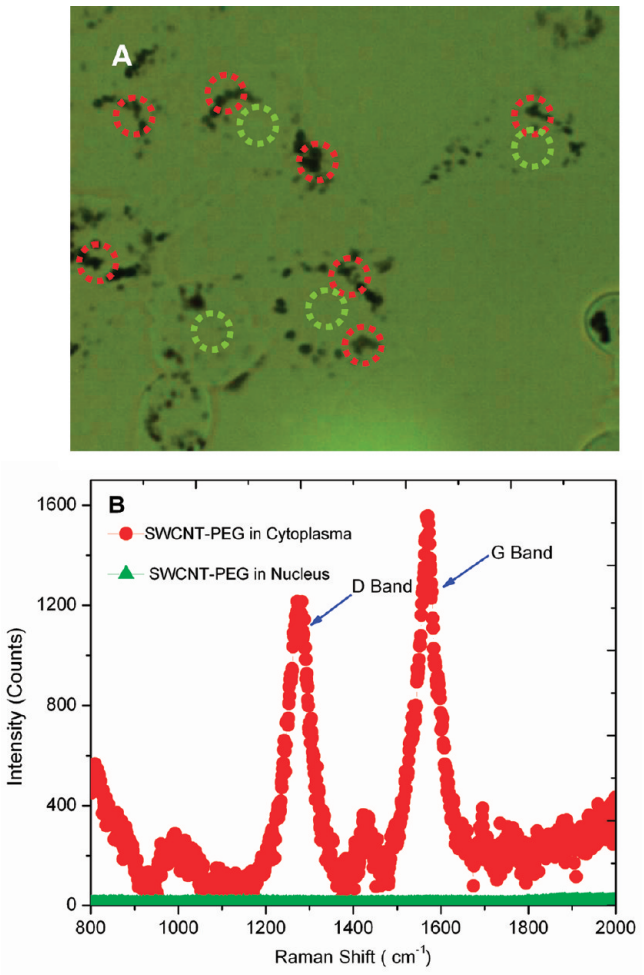

Figure 5. Intracellular distribution of SWCNT-PEGs in PC12 cells. (A) Optical image of PC12 cells that were incubated at 37 °C for 4 h in PEGylated SWCNT dispersion. The colored circles in the optical micrographs represent the specific regions of the PC12 cell where spectra were acquired. (B) Colored Raman spectra acquired from cytoplasmic (red circle) and nuclear (green circle) regions of image (A). SWCNT-PEGs were localized in the cytoplasm evaluated using confocal Raman microscopy after 4 h of exposure to PC12 cells.

uncoated SWCNTs. These results are in line with the already published reports that indicate the role that surface modification plays in nanoparticle cellular uptake, bioactivity, and possible toxic effects.[67] However, the lesser cytotoxicity of SWCNT-PEGs suggested that surface coating of carbon nanotubes with PEG appears to increase the biocompatibility of these organic nanomaterials. These mitochondrial effects and membrane damages can be explained by the surface functionalization of these nanomaterials and their biological interaction with the cellular systems.

The PC12 cells exposed to the SWCNTs appear to take an elongated shape, while SWCNT-PEGs do not seem to have the same effect on cells (Figure 4B,C). The change in the cellular shape induced by the SWCNTs is in good agreement with our previously published studies that showed that osteocytic bone cells change their shape in a similar manner when exposed to SWCNTs.[10] This shape/size change was definitely related to the higher toxic effects induced in cells by the untreated nanotubes. SWCNTs and SWCNT-PEG were found to accumulate in the cells after 4 h of exposure (Figure 5). As previously presented, the "snaking" effects of the SWCNTs, given their tubular shape, promote penetration of various membranes, uptake by cells, and strong interactions with various protein systems.[11] Due to their surface functionalization, the SWCNT-PEG nanostructures were expected to have less interaction with the cellular membranes. It has been reported that different degrees of agglomeration of SWCNTs influence the cell proliferation in primary neuron and glial cells.[32] In our studies, the accumulation of SWCNTs on the cell membranes and cytoplasm after 4 h of incubation may partially contribute to their toxic properties. During these studies (optical microscopy and Raman spectroscopy), we did not observe variations in the amounts of SWCNTs or SWCNT-PEGs that were internalized by the cells, although this is a topic for further investigation.

Toxicity Mechanisms. Several studies have shown that nanomaterials could induce oxidative stress, which may be considered as a biomarker of toxicity to many nanomaterials.[68,69] In biological systems, the oxidation

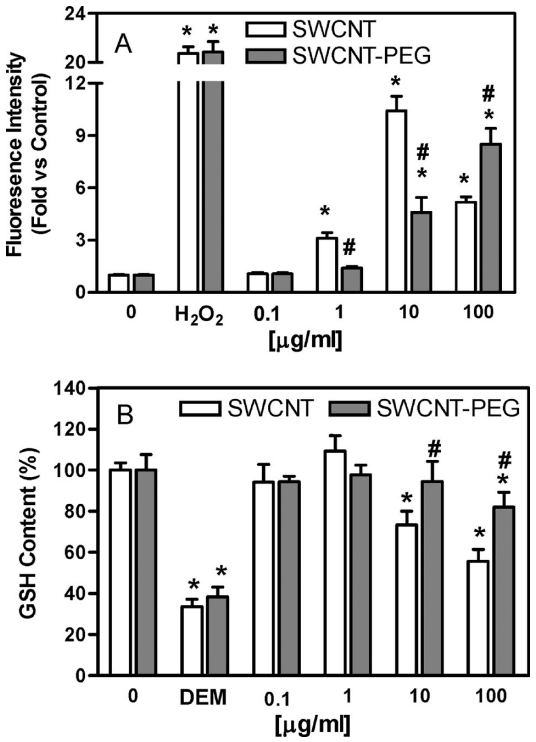

Figure 6. Effect of surface modification of SWCNTs on generation of ROS and GSH levels in PC12 cells. Cells were treated with different concentrations of nanomaterials for 24 h. At the end of the incubation period, ROS or GSH levels were determined as described in the Methods section. Data were expressed as mean ± standard error (SE) based on at least triplicate observations from three independent experiments. (*) indicates statistically significant from control; (#) indicates statistically significant within concentration ($p < 0.05$).

and reduction are coupled processes supported by a group of enzymes known as oxidoreductases. This process involved charged reactive radicals referred to as reactive oxygen species (ROS) such as superoxide ($\bullet O^{2-}$), hydroxyl radicals ($OH\bullet$), and hydrogen peroxide (H_2O_2). ROS, as a short half-life molecule, could be inactivated by antioxidant molecules and associated with the enzymatic activities of oxidoreductases. Although ROS play important roles in maintaining the physiological functions of the body, the persistence of ROS is generally considered harmful. ROS can oxidize macromolecules, such as DNA, proteins, and lipids, resulting in a high degree of cytotoxicity. As a result, the generation of reactive oxygen species was investigated in order to determine the toxic mechanisms that are responsible for the two types of nanomaterials studied in this work: SWCNTs (uncoated) and SWCNT-PEGs. To avoid the potential interference of the carbon nanotubes on this fluorescence assay, cell-free medium with nanoparticles only was used as a control. The nanotubes were neither oxidizing the ROS probe nor quenching the fluorescence by themselves. Figure 6A shows the measured levels of the generated reactive oxygen species to be concentration-dependent after 24 h of cellular exposure to the SWCNTs and SWCNT-PEGs. Surface modification by PEG reduced the capacity of the SWCNTs to generate ROS. Twenty-four hours after treatment, 10 μg/mL of SWCNTs induced a 12-fold increase in ROS as compared to the control samples, while the same dose of SWCNT-PEGs induced only a 5-fold increase in ROS as compared with the controls. On the other hand, 1 μg/mL of SWCNT was found to induce 3-fold ROS compared with the controls, while no detectable increase in ROS was noted for the SWCNT-PEG treatment group in the same concentration. SWCNTs at 100 μg/mL were found to generate substantial cell death based on the LDH release assay, and the intracellular ROS signal decreased compared to the values measured for the lower concentrations of 10 μg/mL of SWCNTs. These data are in agreement with the previous findings that have shown that SWCNTs induce oxidative response in lung epithelial cells at concentrations varying from 1 to 10 μg/mL.[70] Glutathione (GSH), a ubiquitous sulfhydryl containing molecule in cells for maintaining cellular oxidation-reduction homeostasis, can scavenge ROS directly and indirectly, playing an important role in toxicant metabolism.[71] A significant depletion of GSH was noted at 10 and 100 μg/mL of SWCNTs relative to control cells. In contrast, significant cellular GSH changes were observed at 100 μg/mL of SWCNT-PEGs. Taken together, GSH depletion and ROS generation induced by SWCNTs provide solid evidence that the cytotoxicity of SWCNTs is involved in the oxidative stress mechanism.

To further investigate the SWCNT-induced oxidative stress mechanism, the expression of the oxidative stress-related genes was further analyzed. Reverse transcription and real-time PCR array were used in our studies to evaluate 84 genes related to oxidative stress at the same time. Since real-time reverse transcription polymerase chain reaction (RT-PCR) is considered one of the most sensitive and reliable methods for gene expression analysis, this method was used to detect alterations in gene expression levels associated with the toxicity caused by SWCNTs and SWCNT-PEGs in the PC12 cells. ArrayTack, a public array data management and analysis software, was used in this study to analyze and interpret the array data. ArrayTack was developed at the National Center for Toxicology Research (NCTR) of the Food and Drug Administration (FDA) and provided an integrated solution to manage the array data.[72] This software tool provides a convenient approach to normalize the data, examine the data quality, perform statistical analysis, and link significant gene lists to biological databases for functional pathway analysis.[72] In this study, 84 oxidative stress-related genes were examined within one control group and two treatment groups. There were three biological replicates in each group. Hierarchical cluster analysis (HCA) and principle component analysis (PCA) were used to determine the gene

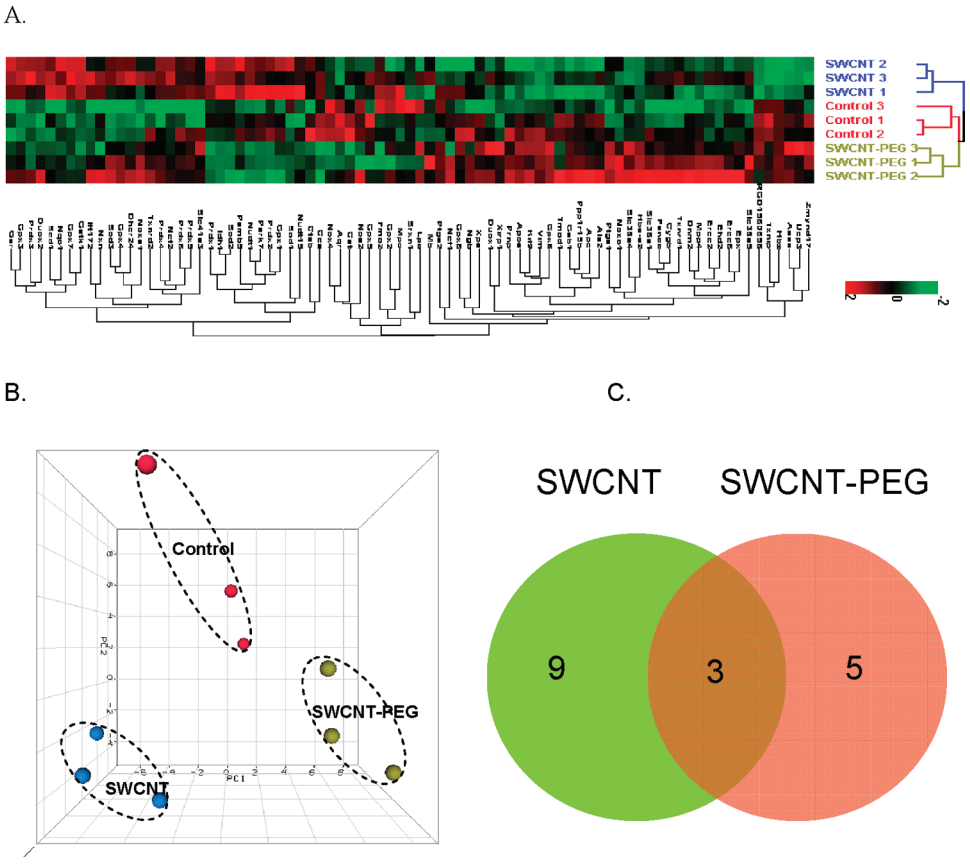

Figure 7. Effect of surface modification of SWCNT on oxidative stress genes. (A) Hierarchical cluster analysis (HCA) and (B) principal component analysis (PCA) of nine array data from PC12 cells treated with SWCNTs, SWCNT-PEGs, and vehicle. Blue dots, yellow dots, and red dots represent the SWCNTs, SWCNT-PEGs, and vehicle-treated samples, respectively. (C) Venn diagram of the gene significantly changed by SWCNT or SWCNT-PEG treatment.

expression profiles for control, SWCNTs, and SWCNT-PEG-treated groups. HCA showed the gene expression was very homogeneous within the SWCNTs, SWCNT-PEGs, and the vehicle treatment group. In other words, there were three clusters according to these treatment groups (Figure 7A). It was not surprising that PCA showed a clear separation among these three treatment groups, indicating that both SWCNT and SWCNT-PEG nanomaterials induced distinct gene expression patterns (Figure 7B). Therefore, the results from HCA and PCA indicate the high-quality and reproducible array data in the study.

Toxicogenomics is focused on patterns of global gene expression as a whole rather than on individual gene expression. When these tools are used to investigate toxicological mechanisms, the resulting outcomes are generally complex, making their interpretation difficult. It should be noted that the fold changes in gene expression may not be proportional to the biological significance and relevance due to the complexity of the signal transduction and amplification process. Slight changes of the upstream gene expression of the signal transduction pathways may cause significant gene changes in the downstream biological processes. In order to identify significantly different expressed gene-related oxidative stress, the criteria of a fold change greater than 1.5 (up or down) and p value less than 0.05 in comparison to the vehicle group were used. With p values of less than 0.05 considered significant, only 3 out of 79 genes were found in common between SWCNT and SWCNT-PEG exposures. In contrast, there were a number of genes (12 out of 79) that were different between SWCNTs and the control group, while 8 out of 79 genes were found to be different between SWCNT-PEGs and the control group, respectively. It should be noted that five genes in the PCR array template set (84 genes) were not expressed in the PC12 cells. It appears that more reduced gene expression changes occur in the PC12 cells after the exposure to SWCNT-PEGs compared with SWCNTs, indicating that distinct gene expression profiles are induced by these two types of carbon nanotubes (Figure 7C). More specifically, the SWCNTs can induce the up-regulation in the expression of the genes involved in ROS metabolism, such as Txnip, Nos2, Ucp3, Nox4, and oxygen transporter gene Hbz, and induce down-regulation in the expression of the ROS metabolism or antioxidant genes, such as Idh1, Dhcr24, Gpx3, Scd1, Gpx7, and Ncf2. However, SWCNT-PEGs induce the down-regulation of ROS-associated oxygen transporter, antioxidant,

TABLE 1. Differentially Expressed Genes Induced by SWCNT or SWCNT-PEG Treatment[a]

		SWCNT		SWCNT-PEG	
symbol	description	*p* value	FC	*p* value	FC
Hbz	hemoglobin, zeta	0.0001	9.61		
RGD1560658	similar to serine (or cysteine) proteinase inhibitor, clade B, member 1b	0.0005	3.54		
Txnip	thioredoxin interacting protein	0.0012	2.99	0.0429	1.53
Nos2	nitric oxide synthase 2, inducible	0.0121	1.74		
Ucp3	uncoupling protein 3 (mitochondrial, proton carrier)	0.0013	1.74		
Nox4	NADPH oxidase 4	0.0018	1.55	0.0047	1.70
Hba-a2	hemoglobin alpha, adult chain 2			0.0025	−1.90
Noxo1	NADPH oxidase organizer 1			0.0111	−1.71
Fancc	Fanconi anemia, complementation group C			0.0324	−1.52
Ptgs1	prostaglandin-endoperoxide synthase 1			0.0072	−2.03
Noxa1	NADPH oxidase activator 1			0.0036	−1.67
Idh1	isocitrate dehydrogenase 1 (NADP+), soluble	0.0041	−1.69		
Dhcr24	24-dehydrocholesterol reductase	0.0234	−1.92	0.0482	−1.70
Gpx3	glutathione peroxidase 3	0.0006	−1.95		
Scd1	stearoyl-coenzyme A desaturase 1	0.0106	−2.04		
Gpx7	glutathione peroxidase 7	0.0028	−2.23		
Ncf2	neutrophil cytosolic factor 2	0.0385	−2.61		

[a] *p* value and fold change were considered as treatment *versus* control group. The genes with *p* value <0.05 and the absolute value of fold change >1.5 were considered as significantly changed.

and ROS metabolism genes, such as Nox4, Hba-a2, Noxo1, Fancc, Ptgs1, Noxa1, and Dhcr24. These distinct gene expression profiles may indicate the unique cellular responses to the exposure to SWCNTs and SWCNT-PEGs (Table 1). It has been reported that intratracheal instillation of 0.5 mg of SWCNTs in mice induced pulmonary alveolar macrophage activation, chronic inflammation responses, and severe pulmonary granuloma formation.[73] Using a human THP-1 derived macrophage model, the authors also found that the uptake of SWCNTs by macrophages resulted in the generation of oxidative stress in mitochondria involved in manganese superoxide dismutase (SOD2) and NADPH-dependent oxidatase (NOXs).[73] Macrophages could take up the SWCNTs with the oxidative responses being directly triggered in cells. In our study, the SWCNTs were found to accumulate in the cell membrane and then migrate to the cytoplasm due to their unique fibrous structure and surface chemistry. The observation of the effect of the mitochondrial function change and mitochondrion gene changes provides evidence of the interactions between the SWCNT and the mitochondrion in PC12 neuronal cells. It has been reported that mitochondria were strongly involved in the generation of the reactive oxygen species, leading to major pathogenicity of many neurodegeneration diseases.[74] Therefore, the uptake and cellular translocation of SWCNTs may partially contribute to the toxicity of the SWCNTs.

Gene ontology analysis provides further evidence for the differential cellular responses of the cells when exposed to SWCNTs and PEGylated SWCNTs. The up-regulated and down-regulated gene functions are shown in Table 2. Genes were up-regulated in most of the categories after exposure to SWCNTs. Many of the genes involve nucleic acid (RNA and DNA) biosynthesis, metabolism, catabolic processes, mitochondria, and oxidoreductases and antioxidant activity. The only down-regulated category was that for the cellular component organization and biogenesis. Collectively, the data suggest an increase in nucleic acid metabolism and biosynthesis, mitochondrial function, and antioxidant activity after the cell responses to oxidative stress, thus resulting in protective adaptation to stress. In contrast, PEGylated SWCNTs result in the up-regulation of lipid metabolic and biosynthetic processes. The PC12 response to the polymer PEG coating is responsible for the lipid biosynthesis, therefore reducing the cytotoxicity. This molecular observation is consistent with the biochemical and cellular responses. The influence of SWCNTs on DNA biosynthesis in our studies is an adaption of the toxicant mechanism. This was evidenced by a previous study in which mixed neuro-glial cultures were exposed to 30 μg/mL SWCNTs, which significantly decreased the overall DNA content when analyzed by using the Hoechst staining assay.[32] Previous findings have reported that 4 or 100 nm PEG-coated gold nanoparticles can induce significant gene expression changes categorized as apoptosis, cell cycle, inflammation, and metabolic processes in mouse liver tissues.[75] Through this analysis, we found that the oxidative damage induced by SWCNTs primarily results from changes in the catabolic process of nucleus acids (DNA and RNA), as well as alteration of mitochondrion functions, while the oxidative damage induced by SWCNT-PEGs is minor. The results of this analysis are consistent with the other findings of this study. The SWCNTs appear to be more

TABLE 2. Gene Functions (gene ontology) Dysregulated by SWCNTs or SWCNTs Coated with PEG ($p < 0.01$)[a]

name	number of genes involved	regulation direction
SWCNT		
response to chemical stimulus	19	up
cellular catabolic process	4	up
catabolic process	4	up
RNA metabolic process	3	up
transcription DNA dependent	3	up
RNA biosynthetic process	3	up
regulation of RNA metabolic process	3	up
biopolymer catabolic process	2	up
DNA catabolic process	2	up
macromolecule catabolic process	2	up
oxidoreductase activity acting on peroxide as acceptor	9	up
antioxidant activity	12	up
system development	6	up
oxidoreductase activity	24	up
regulation of transcription from RNA polymerase II promoter	2	up
Regulation of transcription DNA dependent	2	up
transcription from RNA polymerase II promoter	2	up
mitochondrion	7	up
regulation of cellular component organization and biogenesis	2	down
SWCNT-PEG		
lipid metabolic process	6	up
biosynthetic process	4	up
lipid biosynthetic process	3	up

[a] p values were considered as treatment *versus* control group, and $p < 0.01$ was considered as a significant change of the gene function.

toxic to PC12 cells than SWCNT-PEGs, as demonstrated by the effect of mitochondrial functions and membrane damage. This phenotypic biological response is dose-dependent as well as the capacity to generate oxidative species at the cellular and molecular levels.

On the basis of our studies, a possible mechanism of ROS-mediated toxicity of SWCNT was proposed. SWCNTs were taken up by the PC12 cells and caused upregulation of oxidoreductases, which are involved in 24 oxidative genes. ROS was generated *via* a Fenton reaction with NADP as a cofactor. The lowest level of oxidative stress is associated with the induction of antioxidant and detoxification enzymes such as glutathione. At higher levels of oxidative stress, this protective response is overtaken and depletes the GSH levels, leading to membrane damage and mitochondria cytotoxicity. In contrast, SWCNT-PEGs migrated into PC12 cells and appeared to interact with cells and up-regulate the six genes involved in the lipid metabolic process as demonstrated in our studies. Fewer ROS were also generated, which may be attributed to the surface coating. Therefore, less cell membrane damage and mitochondria function was noted in comparison with uncoated SWCNTs. These studies could be further developed by using flow cytometry analysis to understand the long-term, chronic toxicity effects that are responsible for inducing cellular apoptosis or necrosis. The combination of assays described in this research work proved to have a high sensitivity and clearly indicate the possible undesirable effects induced by materials that have similar sizes and chemical compositions, but different surface chemistry morphologies. On the basis of our results, it can be clearly concluded that the surface properties of nanomaterials play important roles in their corresponding biological responses. Such studies could open the field for the development of low toxicity surface treatment approaches for carbon nanomaterials that could therefore be used in a number of nanomedicine applications ranging from tissue engineering to cancer targeting and destruction.

CONCLUSIONS

Our studies demonstrate that SWCNTs elicit concentration-dependent and surface coating-dependent cytotoxicity in PC12 cells, and cytotoxicity is involved in the oxidative stress mechanism. The surface functionalization of carbon nanomaterials plays an important role in their interaction within biological systems. The differential oxidative stress-mediated toxicity mechanisms of the SWCNTs/SWCNT-PEGs have been shown in this report. In this toxicity evaluation study, the maximum exposure level of nanomaterials may be higher than the practical use of carbon-based nanomaterials in various biomedical applications. However, a lower level of exposure could open the possibility of using nanomaterials with various coatings in advanced biomedical applications. This study performed *in vitro* is the foundation of further *in vivo* studies aimed to elucidate the complex interactions between carbon nanotubes and biological systems and the possible toxic effects given by the size or chemistry of these nanomaterials. Further, it is interesting to study the possible defense mechanisms developed by such biological systems to prevent or minimize the toxic effects of the engineered nanomaterials. Future work will focus on *in vivo* mechanistic toxicity studies at low dose exposure. Given their relatively lower induced toxicity, the surface functionalization of carbon nanotubes is expected to be a promising strategy for delivering drugs and growth factors to neuronal cells with potential in treating major neurodegenerative diseases.

METHODS

SWCNT Synthesis. Carbon nanotubes were synthesized over the Fe–Co/MgO catalyst using the RF-CCVD method and methane as the carbon source.[76] The rf inductive heating was performed using an rf generator operated at a radio frequency of 350 kHz. A 200 mg amount of catalyst was placed in a

graphite boat, and the boat was inserted into a quartz reactor. The catalysts were heated in nitrogen (flow rate of 600 mL/min) and were annealed at 700 °C for 1 h. All of the synthesis reactions were performed at 850 °C with a methane flow rate of 80 mL/min, while keeping the nitrogen flow constant. The temperature of the graphite boat was continuously measured by an optical pyrometer and was found to be very stable during the reaction process. After 30 min of reaction time, the methane was turned off, and the resulting product was allowed to cool in a nitrogen flow. The raw SWCNTs were purified by HCl for 24 h under gentle stirring and washed repeatedly with deionized water. The suspended nanotubes were separated by vacuum-filtration using a 0.22 μm Millipore polycarbonate membrane filter and further washed with water until neutral pH. The resulting CNT sample was dried overnight in a vacuum at 120 °C.

SWCNTs Coated with PEG. SWCNTs were first coated with COOH groups through H_2SO_4/HNO_3 (3:1) treatment. After consecutive washing and drying, $SOCl_2$ was added and mixed with the CNT-COOH powder sample. This reaction was under reflux for 24 h at 70 °C. This process generated COCl-functionalized SWCNTs, which were further mixed with PEG (Bioworld, biotechnology grade, MW = 8000); the mixture was then stirred at 140 °C for 24 h. The resulting solid SWCNT-PEG sample was filtered again through a 0.22 μm Millipore polycarbonate membrane filter and further washed with water. The resulting sample was dried overnight in a vacuum, generating SWCNT-PEG. The SWNT-PEG was dispersed into DI water and then put into a dialysis membrane tubing (cutoff molecular weight is about 12 000) for dialysis to remove the impurities for 2 days before being incubated with cells. The solutions of SWCNT and SWCNT-PEG in cell medium were found to be extremely stable over time and definitely during the duration of the experiments. To exemplify, the SWCNT-PEG solution was found to remain stable at room temperature for over six months without any indication of the agglomeration of the nanotubes. As a result, all of the experiments were performed with nanotubes that were dispersed either individually or in small bundles, as indicated by microscopy studies.

SWCNT and SWCNT-PEG Characterization. Transmission electron microscopy images were collected on a field emission JEM-2100F TEM (JEOL Inc.) equipped with a CCD camera. The acceleration voltage was 100 kV for the SWCNT and SWCNT-PEG analysis. The nanotube samples were homogeneously dispersed in 2-propanol under ultrasonication for 30 min. Next, a few drops of the suspension were deposited on the TEM grid, dried, and evacuated before analysis. EDX elemental analysis was collected on a JEOL-7000 (JEOL Inc.) with an accelerating voltage of 15 kV. The SWCNT sample was mounted on aluminum pins, and the corresponding EDX elemental spectra and data were obtained.

Zetasizer Nano ZS (Malvern Instruments) using dynamic light scattering (DLS) techniques was an ideal tool for characterization of the hydrodynamic size and zeta potential of the nanomaterial in solution. SWCNT or SWCNT-PEG samples were measured after dilution of nanomaterial stock solutions to 100 μg/mL suspensions in RPMI 1640 media. The nanomaterial suspension was vortexed to a homogeneous solution, and 1 mL of suspension was transferred to a plastic cuvette or clear zeta potential cell for measurement following the manufacture's procedure.

Cell Culture. The PC12 cell line obtained from the American Type Culture Collection (Manassas, VA) was maintained at 37 °C (5% CO_2, 95% air) in RPMI-1640 media (Sigma 8758) supplemented with 5% fetal bovine serum (Atlanta Biologicals), 10% horse serum (ATCC), and 1% penicillin/streptomycin (Sigma). Confluent cells were harvested with 0.25% trypsin/EDTA solution (Invitrogen). PC12 cells were allowed to attach on 96-well plates for 48 h before treatment with carbon nanotubes in serum-free, phenol red-free RPMI media.

MTT Assay. The colorimetric MTT (3-(4,5-dimethylthiazol-2-yl)-2,5-diphenyl tetrazolium bromide, Sigma) test assesses cell metabolic activity based on the ability of the mitochondrial succinate/tetrazolium reductase system to convert the yellow dye (MTT) to a purple formazan in living cells. The metabolic activity of the cell is proportional to the color density formed. Briefly, PC12 cells were incubated with various concentrations of SWCNT or SWCNT-PEG for 24 h, then gently washed three times with PBS (pH 7.4) followed by replacement with 90 uL of serum-free medium. To avoid potential interferences of SWCNT in this method, SWCNTs in the medium or attached to the cell membrane were extensively washed. A 10 μL portion of an MTT stock solution (5 mg/mL) was added to each well followed by incubation for 4 h at 37 °C. The supernatant was then removed, and the formazan in cells was dissolved with 100 μL of DMSO. Then the fresh supernatant was transferred to another microplate to read after centrifugation of the plate at 1000*g* for 5 min. The absorbance was determined using a microplate reader (Biotek, USA) at 550 nm with a reference wavelength of 680 nm. H_2O_2 (0.5 mM) was used as a positive control. The subtracted absorbance of cell free blank was calculated, and data are presented as percent survival of control cells.

XTT Assay. The cell viability of PC12 cells following exposure to SWCNT or SWCNT-PEG was determined by measuring the mitochondrial-dependent reduction of colorless 2,3-bis[2-methoxy-4-nitro-5-sulfophenyl]-2*H*-tetrazolium-5-carboxanilide (XTT) to a soluble, orange-colored formazan derivative. Briefly, the cells were seeded in a 96-well cell culture plate at a density of 1×10^5 cells/mL in 100 μL of growth media and cultured for 48 h. The cells were treated with different concentrations of SWCNT or SWCNT-PEG for 24 h, then gently washed three times with PBS (pH 7.4), supplied with fresh growth media (150 μL/well) containing fresh XTT reagent (300 $\mu g/cm^3$) and phenazine methosulfate (37.5 μM final concentration), and further incubated for 2 h at ambient temperature. H_2O_2 (0.5 mM) was used as a positive control in this experiment. The absorbance was determined using a microplate reader (Biotek, USA) at 450 nm with a reference wavelength of 680 nm. The absorbance data were analyzed and corrected for interference by subtracting absorbance of the nanomaterials and cells prior to the addition of XTT reagents. The subtracted absorbance of control cells (nanoparticle free media) was calculated, and data are presented as percent survival of control cells.

LDH Assay. Cell membrane integrity can be measured by lactate dehydrogenase (LDH) leakage assay. LDH leakage was measured using a cytotoxicity detection kit (Roche Applied Science). Extracelluar LDH was measured with a coupled enzymatic assay that results in the conversion of a tetrazolium salt (INT) into a red formazan product. In this experiment, PC12 cells cultured with 1% Triton-X-100 were used as positive control, and cells cultured in nanoparticle-free media were used as negative control. Media with each sample only were set as respective cell-free blank control. PC12 cells (1×10^5 cells/mL) were treated at 100 μL of different concentrations of SWCNT or SWCNT-PEG nanomaterials or positive control 1% Triton-x-100 for 24 h. Then 50 μL of supernatant was transferred to another plate followed by the addition of 50 μL of substrate mix. The plate was incubated for 30 min at room temperature followed by the addition of 50 μL of stop solution to each well. Absorbance was recorded at 490 nm in a plate reader (Biotek, USA) using a reference wavelength of 680 nm. LDH leakage was calculated using the following formulation: LDH leakage (%) = 100[(sample absorbance − cell free sample blank) − mean media control absorbance]/(mean Ttriton-X-100 positive control absorbance − mean media control absorbance).

Measurement of Reactive Oxygen Species. The intracellular reactive oxygen species level was detected using DCFH-DA (Molecule Probes Inc., Eugene, OR). DCFH-DA is ROS probe that undergoes intracellular deacetylation, followed by ROS-mediated oxidation to fluorescent species. DAFH-DA can be used to measure ROS generation in the cytoplasm and cellular organelles, such as mitochondria. In this experiment, PC12 cells cultured with nanoparticle-free media were used as control. Media with each sample only were set as respective cell-free blank control. Briefly, the cells were seeded in a 96-well cell culture plate at a density of 1×10^5 cells/mL in 100 μL of growth media and cultured for 48 h. PC12 cells were gently washed three times with PBS (pH 7.4) and then incubated with DCFH-DA (100 μM) in medium for 30 min. PC12 cells were again washed three times with phosphate-buffered saline solution and then cultured with various concentrations of SWCNT or SWCNT-PEG. The

fluorescence intensity (indicating ROS levels) of the cells was determined 24 h after the treatment using a plate reader with an excitation/emission wavelength of 485 nm/530 nm (Biotek, USA). The values were analyzed and corrected for interference by subtracting the value of the nanomaterials and cells (blank control). H_2O_2 (10 μM) was used as a positive control in this experiment. The values were expressed as a percent of relative fluorescent units to positive control wells. All of the procedures were performed without exposure to light.

Measurement of GSH Content. The content of GSH was determined using the GSH-Glo Glutathione Assay kit from Preomega (Madison, WI) according to the manufacturer's protocol. The assay is based on the conversion of a luciferin derivative into luciferin in the presence of glutathione, catalyzed by glutathione S-transferase. The signal generated in a coupled reaction with firefly luciferase is proportional to the amount of glutathione present in the sample. Briefly, PC12 cells were plated at 10 000 cells/well in a 96-well plate or 1.5×10^5/well in a six-well plate and allowed to attach for 48 h. Various amounts of SWCNT or SWCNT-PEG were added, and the cells were incubated for 24 h. The medium was removed from wells in 96-well plates, and 100 μL of GSH-Glo Reagent was added. A GSH standard curve was generated at the same time as described in the manufacturer's protocol. Media with each sample only were set as respective cell-free assay controls to evaluate if the carbon nanomaterials interfere with the approach. Diethyl maleate (0.5 mM) was used in this study as a positive control. The reaction was stopped by adding 100 μL of Luciferin Detection Reagent, and luminescence was measured after 15 min. The amount of GSH was calculated on the basis of the standard curve. The cells in six-well plates were harvested after 24 h exposure followed by the standard Bradford Protein assay (Bio-Rad, CA). The glutathione content was normalized as μmol/mg protein. Control cells (9.43 μmol/mg) were used. Data are presented as percent GSH content of control cells.

Dark-Field Microscopy Imaging. To evaluate possible morphological changes induced by SWCNT or SWCNT-PEG in the cell culture, SWCNTs or SWCNT-PEGs (10 μg/mL) were incubated with PC12 cells on collagen-coated coverslips lying in the six-well plate for up to 24 h. The medium was removed, and the PC12 cells were rinsed three times with sterile PBS. The coverslip containing cells was sealed on the glass slide using nail polish. Images were captured using a dark-field microscope (Cytoviva Inc.).

Confocal Raman Microscopy. Raman scattering spectra of the SWCNTs and SWCNT-PEGs were acquired at room temperature using a Horiba Jobin Yvon high-resolution LabRam Raman microscope system equipped with a charge-coupled detector and a spectrometer with a grating of 600 lines/mm. The systems were set up with a 150 μm entrance slit and a 400 μm pinhole. The 633 nm laser excitation was provided by a helium−neon laser operating at 5 mW. Raman shift calibration was performed using the 521 cm^{-1} line of a silicon wafer. In the cellular distribution study, adherent cells in a coverslip were brought into focus by transmitted white-light images obtained through a CCD video camera followed by Raman spectra collection. All spectra were plotted as the average of three scans.

RNA Isolation. Total RNA was isolated with a mirVana miRNA isolation kit (Ambion Inc., Austin, TX) from cells treated with either 10 μg/mL SWCNT, SWCNT-PEG, or vehicle by following the total RNA isolation procedure suggested by the manufacturer. The quality and quantity of RNA were measured by a Nanodrop ND-1000 spectrophotometer (Nanodrop Technologies, Rockland, DE). All of the RNA samples have an OD260/280 ratio > 1.9, indicating the high quality of RNA.

Reverse Transcription and Real-Time PCR Array. Total RNA samples were analyzed using an RT^2 Profiler PCR Array System (SABioscience, Frederick, MD, #PARN-065C). The first strand synthesis was carried out by the RT^2 PCR Array First Strand kit followed by real-time PCR with Oxidative Stress RT^2 Profiler PCR Array on an ABI 7500 PCR machine (Applied Biosystems Inc., Foster, CA). The thermo cycler parameters were set up as follows: 95 °C for 10 min, 40 cycles of 95 °C for 15 s, and 60 °C for 1 min.

PCR Array Analysis. The PCR array data were analyzed using PCR array data analysis software provided by SABiosciences. The raw Ct was extracted by 7500 software V2.0 (Applied Biosystems) by setting the threshold line as 0.15. The baseline was automatically determined by the software. The PCR array system contains built-in positive control elements for the proper normalization of the data, for the detection of genomic DNA contamination, for the quality of the RNA samples, and for general PCR performance. Normalization was conducted by subtracting the mean Ct value of five house-keeping genes, Rplp1, Hprt1, Rpl13a, Ldha, and Actb, from the raw Ct value of each gene present in the PCR array. *p*-Values and fold changes were calculated by *t* test and the $\Delta\Delta$Ct method, respectively. Gene expression was considered significantly changed when the fold change was ≥ 1.5 and $p \leq 0.05$. The normalized Ct values were input into an Array Track database (NCTR, Jefferson, AR) for principle-component analysis and hierarchical cluster analysis. Functional analysis was carried out by GSEA software.

Statistical Analyses. Cytotoxicity data were expressed as mean $\pm$ standard error based on at least triplicate observations from three independent experiments. Statistical significance was determined by two-way analysis of variance (ANOVA) followed by Dunnett's multiple comparison test. A value of $p < 0.05$ was considered statistically significant. The analyses were conducted using the Prism software package (GraphPad Software).

Acknowledgment. This research was supported in part by an appointment (Y.Z.) to the Research Participation Program at the National Center for Toxicological Research administered by the Oak Ridge Institute of Science and Education through an interagency agreement between the U.S. Department of Energy and the U.S. Food and Drug Administration. Portions of these studies were conducted using the Nanotechnology Core Facility (NanoCore) located at the U.S. Food & Drug Administration's National Center for Toxicological Research (NCTR) and Office of Regulatory Affairs Arkansas Regional Laboratory (ORA/ARL) campus. The views presented in this article do not necessarily reflect those of the U.S. Food and Drug Administration. The financial support of the U.S. Army Telemedicine and Advanced Research Center program is highly appreciated. The editorial assistance of Dr. Marinelle Ringer is also acknowledged.

REFERENCES AND NOTES

1. Kang, S. J.; Kocabas, C.; Ozel, T.; Shim, M.; Pimparkar, N.; Alam, M. A.; Rotkin, S. V.; Rogers, J. A. High-performance Electronics Using Dense, Perfectly Aligned Arrays of Single-walled Carbon Nanotubes. *Nat. Nanotechnol.* **2007**, *2*, 230–236.
2. Rao, S. G.; Huang, L.; Setyawan, W.; Hong, S. Nanotube Electronics: Large-Scale Assembly of Carbon Nanotubes. *Nature* **2003**, *425*, 36–37.
3. Hill, F. A.; Havel, T. F.; Livermore, C. Modeling Mechanical Energy Storage in Springs Based on Carbon Nanotubes. *Nanotechnology* **2009**, *20*, 255704–255715.
4. Welsher, K.; Liu, Z.; Daranciang, D.; Dai, H. Selective Probing and Imaging of Cells with Single Walled Carbon Nanotubes as Near-infrared Fluorescent Molecules. *Nano Lett.* **2008**, *8*, 586–590.
5. Barone, P. W.; Baik, S.; Heller, D. A.; Strano, M. S. Near-infrared Optical Sensors Based on Single-Walled Carbon Nanotubes. *Nat. Mater.* **2005**, *4*, 86–92.
6. De la Zerda, A.; Zavaleta, C.; Keren, S.; Vaithilingam, S.; Bodapati, S.; Liu, Z.; Levi, J.; Smith, B. R.; Ma, T. J.; Oralkan, O.; *et al*. Carbon Nanotubes as Photoacoustic Molecular Imaging Agents in Living Mice. *Nat. Nanotechnol.* **2008**, *3*, 557–562.
7. Kim, J. W.; Galanzha, E. I.; Shashkov, E. V.; Moon, H. M.; Zharov, V. P. Golden Carbon Nanotubes as Multimodal Photoacoustic and Photothermal High-Contrast Molecular Agents. *Nat. Nanotechnol.* **2009**, *4*, 688–694.
8. Feazell, R. P.; Nakayama-Ratchford, N.; Dai, H.; Lippard, S. J. Soluble Single-Walled Carbon Nanotubes as Longboat Delivery Systems for Platinum(IV) Anticancer Drug Design. *J. Am. Chem. Soc.* **2007**, *129*, 8438–8439.
9. Mahmood, M.; Karmakar, A.; Fejleh, A.; Mocan, T.; Iancu, C.; Mocan, L.; Iancu, D. T.; Xu, Y.; Dervishi, E.; Li, Z.; *et al*. Synergistic Enhancement of Cancer Therapy Using a

Combination of Carbon Nanotubes and Anti-tumor Drug. *Nanomedicine (London)* **2009**, *4*, 883–893.
10. Mahmood, M.; Casciano, D. A.; Mocan, T.; Iancu, C.; Xu, Y.; Mocan, L.; Iancu, D. T.; Dervishi, E.; Li, Z.; Abdalmuhsen, M.; *et al*. Cytotoxicity and Biological Effects of Functional Nanomaterials Delivered to Various Cell Lines. *J. Appl. Toxicol.* **2010**, *30*, 74–83.
11. Zhang, Y.; Ali, S. F.; Dervishi, E.; Xu, Y.; Li, Z.; Casciano, D.; Biris, A. S. Cytotoxicity Effects of Graphene and Single-Wall Carbon Nanotubes in Neural Phaeochromocytoma-Derived PC12 Cells. *ACS Nano* **2010**, *4*, 3181–3186.
12. Khodakovskaya, M. V.; de Silva, K.; Nedosekin, D. A.; Dervishi, E.; Biris, A. S.; Shashkov, E. V.; Galanzha, E. I.; Zharov, V. P. Complex Genetic, Photothermal, and Photoacoustic Analysis of Nanoparticle-Plant Interactions. *Proc. Natl. Acad. Sci. U. S. A.* **2011**, *108*, 1028–1033.
13. Zhang, Y.; Bai, Y.; Yan, B. Functionalized Carbon Nanotubes for Potential Medicinal Applications. *Drug Discovery Today* **2010**, *15*, 428–435.
14. Albertorio, F.; Hughes, M. E.; Golovchenko, J. A.; Branton, D. Base Dependent DNA-Carbon Nanotube Interactions: Activation Enthalpies and Assembly-Disassembly Control. *Nanotechnology* **2009**, *20*, 395101–395110.
15. Zheng, M.; Jagota, A.; Semke, E. D.; Diner, B. A.; McLean, R. S.; Lustig, S. R.; Richardson, R. E.; Tassi, N. G. DNA-Assisted Dispersion and Separation of Carbon Nanotubes. *Nat. Mater.* **2003**, *2*, 338–342.
16. Singh, I.; Rehni, A. K.; Kumar, P.; Kumar, M.; Aboul-Enein, H. Y. Carbon Nanotubes: Synthesis, Properties and Pharmaceutical Applications. *Fullerenes Nanotubes and Carbon Nanostruct.* **2009**, *17*, 361–377.
17. Bianco, A.; Kostarelos, K.; Partidos, C. D.; Prato, M. Biomedical Applications of Functionalised Carbon Nanotubes. *Chem Commun. (Cambridge, U.K.)* **2005**, 571–577.
18. Karmakar, A.; Bratton, S. M.; Dervishi, E.; Ghosh, A.; Mahmood, M.; Xu, Y.; Saeed, L. M.; Mustafa, T.; Casciano, D.; Radominska-Pandya, A.; *et al*. Ethylenediamine Functionalized-Single-Walled Nanotube (f-SWNT)-Assisted *In Vitro* Delivery of the Oncogene Suppressor p53 Gene to Breast Cancer MCF-7 Cells. *Int. J. Nanomed.* **2011**, *6*, 1045–1055.
19. Lee, H. J.; Park, J.; Yoon, O. J.; Kim, H. W.; Lee do, Y.; Kim do, H.; Lee, W. B.; Lee, N. E.; Bonventre, J. V.; Kim, S. S. Amine-Modified Single-Walled Carbon Nanotubes Protect Neurons from Injury in a Rat Stroke Model. *Nat. Nanotechnol.* **2011**, *6*, 121–125.
20. Li, X. M.; Fan, Y. B.; Watari, F. Current Investigations into Carbon Nanotubes for Biomedical Application. *Biomedical Materials* **2010**, *5*, 022001–022012.
21. Liu, Z.; Chen, K.; Davis, C.; Sherlock, S.; Cao, Q.; Chen, X.; Dai, H. Drug Delivery with Carbon Nanotubes for *In Vivo* Cancer Treatment. *Cancer Res.* **2008**, *68*, 6652–6660.
22. Yan, L.; Zhao, F.; Li, S.; Hu, Z.; Zhao, Y. Low-toxic and Safe Nanomaterials by Surface-Chemical Design, Carbon Nanotubes, Fullerenes, Metallofullerenes, and Graphenes. *Nanoscale* **2011**, *3*, 362–382.
23. Kagan, V. E.; Konduru, N. V.; Feng, W.; Allen, B. L.; Conroy, J.; Volkov, Y.; Vlasova, I. I.; Belikova, N. A.; Yanamala, N.; Kapralov, A.; *et al*. Carbon Nanotubes Degraded by Neutrophil Myeloperoxidase Induce Less Pulmonary Inflammation. *Nat. Nanotechnol.* **2010**, *5*, 354–359.
24. Rivera Gil, P.; Oberdorster, G.; Elder, A.; Puntes, V.; Parak, W. J. Correlating Physico-chemical with Toxicological Properties of Nanoparticles: The Present and the Future. *ACS Nano* **2010**, *4*, 5527–5531.
25. Schipper, M. L.; Nakayama-Ratchford, N.; Davis, C. R.; Kam, N. W.; Chu, P.; Liu, Z.; Sun, X.; Dai, H.; Gambhir, S. S. A Pilot Toxicology Study of Single-Walled Carbon Nanotubes in a Small Sample of Mice. *Nat. Nanotechnol.* **2008**, *3*, 216–221.
26. Liu, Z.; Davis, C.; Cai, W.; He, L.; Chen, X.; Dai, H. Circulation and Long-Term Fate of Functionalized, Biocompatible Single-Walled Carbon Nanotubes in Mice Probed by Raman Spectroscopy. *Proc. Natl. Acad. Sci. U. S. A.* **2008**, *105*, 1410–1415.
27. Chen, X.; Tam, U. C.; Czlapinski, J. L.; Lee, G. S.; Rabuka, D.; Zettl, A.; Bertozzi, C. R. Interfacing Carbon Nanotubes with Living Cells. *J. Am. Chem. Soc.* **2006**, *128*, 6292–6293.
28. Chin, S. F.; Baughman, R. H.; Dalton, A. B.; Dieckmann, G. R.; Draper, R. K.; Mikoryak, C.; Musselman, I. H.; Poenitzsch, V. Z.; Xie, H.; Pantano, P. Amphiphilic Helical Peptide Enhances the Uptake of Single-Walled Carbon Nanotubes by Living Cells. *Exp. Biol. Med. (Maywood, N.J., U.S.)* **2007**, *232*, 1236–1244.
29. Dumortier, H.; Lacotte, S.; Pastorin, G.; Marega, R.; Wu, W.; Bonifazi, D.; Briand, J. P.; Prato, M.; Muller, S.; Bianco, A. Functionalized Carbon Nanotubes are Non-cytotoxic and Preserve the Functionality of Primary Immune Cells. *Nano Lett.* **2006**, *6*, 1522–1528.
30. Kam, N. W.; O'Connell, M.; Wisdom, J. A.; Dai, H. Carbon Nanotubes as Multifunctional Biological Transporters and Near-infrared Agents for Selective Cancer Cell Destruction. *Proc. Natl. Acad. Sci. U. S. A.* **2005**, *102*, 11600–11605.
31. Liu, Z.; Sun, X.; Nakayama-Ratchford, N.; Dai, H. Supramolecular Chemistry on Water-Soluble Carbon Nanotubes for Drug Loading and Delivery. *ACS Nano* **2007**, *1*, 50–56.
32. Belyanskaya, L.; Weigel, S.; Hirsch, C.; Tobler, U.; Krug, H. F.; Wick, P. Effects of Carbon Nanotubes on Primary Neurons and Glial Cells. *Neurotoxicology* **2009**, *30*, 702–711.
33. Hirano, S.; Kanno, S.; Furuyama, A. Multi-walled Carbon Nanotubes Injure the Plasma Membrane of Macrophages. *Toxicol. Appl. Pharmacol.* **2008**, *232*, 244–251.
34. Kisin, E. R.; Murray, A. R.; Keane, M. J.; Shi, X. C.; Schwegler-Berry, D.; Gorelik, O.; Arepalli, S.; Castranova, V.; Wallace, W. E.; Kagan, V. E.; *et al*. Single-Walled Carbon Nanotubes: Geno- and Cytotoxic Effects in Lung Fibroblast V79 Cells. *J. Toxicol. Environ. Health A* **2007**, *70*, 2071–2079.
35. Murray, A. R.; Kisin, E.; Leonard, S. S.; Young, S. H.; Kommineni, C.; Kagan, V. E.; Castranova, V.; Shvedova, A. A. Oxidative Stress and Inflammatory Response in Dermal Toxicity of Single-Walled Carbon Nanotubes. *Toxicology* **2009**, *257*, 161–171.
36. Walker, V. G.; Li, Z.; Hulderman, T.; Schwegler-Berry, D.; Kashon, M. L.; Simeonova, P. P. Potential *in Vitro* Effects of Carbon Nanotubes on Human Aortic Endothelial Cells. *Toxicol. Appl. Pharmacol.* **2009**, *236*, 319–328.
37. Zhu, L.; Chang, D. W.; Dai, L.; Hong, Y. DNA Damage Induced by Multiwalled Carbon Nanotubes in Mouse Embryonic Stem Cells. *Nano Lett.* **2007**, *7*, 3592–3597.
38. Warheit, D. B.; Laurence, B. R.; Reed, K. L.; Roach, D. H.; Reynolds, G. A.; Webb, T. R. Comparative Pulmonary Toxicity Assessment of Single-Wall Carbon Nanotubes in Rats. *Toxicol. Sci.* **2004**, *77*, 117–125.
39. Mitchell, L. A.; Lauer, F. T.; Burchiel, S. W.; McDonald, J. D. Mechanisms for How Inhaled Multiwalled Carbon Nanotubes Suppress Systemic Immune Function in Mice. *Nat. Nanotechnol.* **2009**, *4*, 451–456.
40. Lam, C. W.; James, J. T.; McCluskey, R.; Hunter, R. L. Pulmonary Toxicity of Single-Wall Carbon Nanotubes in Mice 7 and 90 Days after Intratracheal Instillation. *Toxicol. Sci.* **2004**, *77*, 126–134.
41. Muller, J.; Huaux, F.; Moreau, N.; Misson, P.; Heilier, J. F.; Delos, M.; Arras, M.; Fonseca, A.; Nagy, J. B.; Lison, D. Respiratory Toxicity of Multi-wall Carbon Nanotubes. *Toxicol. Appl. Pharmacol.* **2005**, *207*, 221–231.
42. Ma-Hock, L.; Treumann, S.; Strauss, V.; Brill, S.; Luizi, F.; Mertler, M.; Wiench, K.; Gamer, A. O.; van Ravenzwaay, B.; Landsiedel, R. Inhalation Toxicity of Multiwall Carbon Nanotubes in Rats Exposed for 3 Months. *Toxicol. Sci.* **2009**, *112*, 468–481.
43. Yang, S. T.; Wang, X.; Jia, G.; Gu, Y.; Wang, T.; Nie, H.; Ge, C.; Wang, H.; Liu, Y. Long-Term Accumulation and Low Toxicity of Single-Walled Carbon Nanotubes in Intravenously Exposed Mice. *Toxicol. Lett.* **2008**, *181*, 182–189.
44. Groten, J. P.; Sinkeldam, E. J.; Muys, T.; Luten, J. B.; Vanbladeren, P. J. Interaction of Dietary Ca, P, Mg, Mn, Cu, Fe, Zn and Se with the Accumulation and Oral Toxicity of Cadmium in Rats. *Food Chem. Toxicol.* **1991**, *29*, 249–258.
45. Poland, C. A.; Duffin, R.; Kinloch, I.; Maynard, A.; Wallace, W. A.; Seaton, A.; Stone, V.; Brown, S.; Macnee, W.;

Donaldson, K. Carbon Nanotubes Introduced into the Abdominal Cavity of Mice Show Asbestos-like Pathogenicity in a Pilot Study. *Nat. Nanotechnol.* **2008**, *3*, 423–428.
46. Hussain, S. M.; Javorina, A. K.; Schrand, A. M.; Duhart, H. M.; Ali, S. F.; Schlager, J. J. The Interaction of Manganese Nanoparticles with PC-12 Cells Induces Dopamine Depletion. *Toxicol. Sci.* **2006**, *92*, 456–463.
47. Wang, J.; Rahman, M. F.; Duhart, H. M.; Newport, G. D.; Patterson, T. A.; Murdock, R. C.; Hussain, S. M.; Schlager, J. J.; Ali, S. F. Expression Changes of Dopaminergic System-Related Genes in PC12 Cells Induced by Manganese, Silver, or Copper Nanoparticles. *Neurotoxicology* **2009**, *30*, 926–933.
48. Elder, A.; Gelein, R.; Silva, V.; Feikert, T.; Opanashuk, L.; Carter, J.; Potter, R.; Maynard, A.; Ito, Y.; Finkelstein, J.; *et al*. Translocation of Inhaled Ultrafine Manganese Oxide Particles to the Central Nervous System. *Environ. Health Perspect.* **2006**, *114*, 1172–1178.
49. Oberdorster, E. Manufactured Nanomaterials (Fullerenes, C60) Induce Oxidative Stress in the Brain of Juvenile Largemouth Bass. *Environ. Health Perspect.* **2004**, *112*, 1058–1062.
50. Yang, S. T.; Guo, W.; Lin, Y.; Deng, X. Y.; Wang, H. F.; Sun, H. F.; Liu, Y. F.; Wang, X.; Wang, W.; Chen, M.; *et al*. Biodistribution of Pristine Single-Walled Carbon Nanotubes. *In Vivo. J. Phys. Chem. C* **2007**, *111*, 17761–17764.
51. Liu, Z.; Cai, W.; He, L.; Nakayama, N.; Chen, K.; Sun, X.; Chen, X.; Dai, H. *In Vivo* Biodistribution and Highly Efficient Tumour Targeting of Carbon Nanotubes in Mice. *Nat. Nanotechnol.* **2007**, *2*, 47–52.
52. Liu, S.; Xu, L.; Zhang, T.; Ren, G.; Yang, Z. Oxidative Stress and Apoptosis Induced by Nanosized Titanium Dioxide in PC12 Cells. *Toxicology* **2010**, *267*, 172–177.
53. Wu, J.; Wang, C.; Sun, J.; Xue, Y., Neurotoxicity of Silica Nanoparticles: Brain Localization and Dopaminergic Neurons Damage Pathways. *ACS Nano* **2011**, *5* (6), 4476−4489.
54. Powers, C. M.; Badireddy, A. R.; Ryde, I. T.; Seidler, F. J.; Slotkin, T. A. Silver Nanoparticles Compromise Neurodevelopment in PC12 Cells: Critical Contributions of Silver Ion, Particle Size, Coating, and Composition. *Environ. Health Perspect.* **2011**, *119*, 37–44.
55. Kim, J. A.; Lee, N.; Kim, B. H.; Rhee, W. J.; Yoon, S.; Hyeon, T.; Park, T. H. Enhancement of Neurite Outgrowth in PC12 Cells by Iron Oxide Nanoparticles. *Biomaterials* **2011**, *32*, 2871–2877.
56. Neibert, K. D.; Maysinger, D. Mechanisms of Cellular Adaptation to Quantum Dots - The Role of Glutathione and Transcription Factor EB. *Nanotoxicology* **2011**. doi: 10.3109/17435390.2011.572195.
57. Wu, J.; Sun, J.; Xue, Y. Involvement of JNK and P53 Activation in G2/M Cell Cycle Arrest and Apoptosis Induced by Titanium Dioxide Nanoparticles in Neuron Cells. *Toxicol. Lett.* **2010**, *199*, 269–276.
58. Biris, A. S.; Galanzha, E. I.; Li, Z.; Mahmood, M.; Xu, Y.; Zharov, V. P. *In Vivo* Raman Flow Cytometry for Real-Time Detection of Carbon Nanotube Kinetics in Lymph, Blood, and Tissues. *J. Biomed. Opt.* **2009**, *14*, 021006–021010.
59. Warheit, D. B. How Meaningful are the Results of Nanotoxicity Studies in the Absence of Adequate Material Characterization? *Toxicol. Sci.* **2008**, *101*, 183–185.
60. Dresselhaus, M. S.; Dresselhaus, G.; Jorio, A.; Souza Filho, A. G.; Samsonidze, G. G.; Saito, R. Science and Applications of Single-Nanotube Raman Spectroscopy. *J. Nanosci. Nanotechnol.* **2003**, *3*, 19–37.
61. Buisson, J. P.; Chauvet, O.; Lefant, S.; Stephan, C.; Benoit, J. M. In Surrounding Effects in Single-walled and Multi-walled Carbon Nanotubes. *Mater. Res. Symp. Proc.* **2001**, *633*, A14.12.1.
62. Hillegass, J. M.; Shukla, A.; Lathrop, S. A.; MacPherson, M. B.; Fukagawa, N. K.; Mossman, B. T. Assessing Nanotoxicity in Cells *In Vitro*. *Wiley Interdiscip. Rev. Nanomed. Nanobiotechnol.* **2010**, *2*, 219–231.
63. Worle-Knirsch, J. M.; Pulskamp, K.; Krug, H. F. Oops They Did It Again! Carbon Nanotubes Hoax Scientists in Viability Assays. *Nano Lett.* **2006**, *6*, 1261–1268.
64. Coccini, T.; Roda, E.; Sarigiannis, D. A.; Mustarelli, P.; Quartarone, E.; Profumo, A.; Manzo, L. Effects of Water-Soluble Functionalized Multi-walled Carbon Nanotubes Examined by Different Cytotoxicity Methods in Human Astrocyte D384 and Lung A549 Cells. *Toxicology* **2010**, *269*, 41–53.
65. Vittorio, O.; Raffa, V.; Cuschieri, A. Influence of Purity and Surface Oxidation on Cytotoxicity of Multiwalled Carbon Nanotubes with Human Neuroblastoma Cells. *Nanomedicine* **2009**, *5*, 424–431.
66. Fotakis, G.; Timbrell, J. A. In Vitro Cytotoxicity Assays: Comparison of LDH, Neutral Red, MTT and Protein Assay in Hepatoma Cell Lines Following Exposure to Cadmium Chloride. *Toxicol. Lett.* **2006**, *160*, 171–177.
67. Win, K. Y.; Feng, S. S. Effects of Particle Size and Surface Coating on Cellular Uptake of Polymeric Nanoparticles for Oral Delivery of Anticancer Drugs. *Biomaterials* **2005**, *26*, 2713–2722.
68. Shi, L.; Hernandez, B.; Selke, M. Singlet Oxygen Generation from Water-Soluble Quantum Dot−Organic Dye Nanocomposites. *J. Am. Chem. Soc.* **2006**, *128*, 6278–6279.
69. Nel, A.; Xia, T.; Madler, L.; Li, N. Toxic Potential of Materials at the Nano Level. *Science* **2006**, *311*, 622–627.
70. Sharma, C. S.; Sarkar, S.; Periyakaruppan, A.; Barr, J.; Wise, K.; Thomas, R.; Wilson, B. L.; Ramesh, G. T. Single-Walled Carbon Nanotubes Induce Oxidative Stress in Rat Lung Epithelial Cells. *J. Nanosci. Nanotechnol.* **2007**, *7*, 2466–2472.
71. Sies, H. Glutathione and Its Role in Cellular Functions. *Free Radical Biol. Med.* **1999**, *27*, 916–921.
72. Tong, W.; Harris, S.; Cao, X.; Fang, H.; Shi, L.; Sun, H.; Fuscoe, J.; Harris, A.; Hong, H.; Xie, Q.; *et al*. Development of Public Toxicogenomics Software for Microarray Data Management and Analysis. *Mutat. Res.* **2004**, *549*, 241–253.
73. Chou, C. C.; Hsiao, H. Y.; Hong, Q. S.; Chen, C. H.; Peng, Y. W.; Chen, H. W.; Yang, P. C. Single-Walled Carbon Nanotubes Can Induce Pulmonary Injury in Mouse Model. *Nano Lett.* **2008**, *8*, 437–445.
74. Lenaz, G.; Bovina, C.; Formiggini, G.; Parenti Castelli, G. Mitochondria, Oxidative Stress, and Antioxidant Defences. *Acta. Biochim. Polym.* **1999**, *46*, 1–21.
75. Cho, W. S.; Kim, S.; Han, B. S.; Son, W. C.; Jeong, J. Comparison of Gene Expression Profiles in Mice Liver Following Intravenous Injection of 4 and 100 nm-sized PEG-Coated Gold Nanoparticles. *Toxicol. Lett.* **2009**, *191*, 96–102.
76. Xu, Y.; Li, Z. R.; Dervishi, E.; Saini, V.; Cui, J. B.; Biris, A. R.; Lupu, D.; Biris, A. S. Surface Area and Thermal Stability Effect of the MgO Supported Catalysts for the Synthesis of Carbon Nanotubes. *J. Mater Chem.* **2008**, *18*, 5738–5745.